Automated approach to measure pulmonary nodule volume based on radius and CT number

Tatsuro Hayashi[1], Xiangrong Zhou[1], and Hiroshi Fujita[1]

[1] Department of Intelligent Image Information, Graduate School of Medicine,
Gifu University, 1-1 Yanagido, Gifu 501-1194, Japan
{hayashi, zxr, fujita} @fjt.info.gifu-u.ac.jp

Abstract. Determining the change in the pulmonary nodule size is a critical measurement for cancer diagnosis and therapy evaluation. In this study, an image-processing method that quantifies the nodule volume change based on computed tomography (CT) images is proposed. The proposed method consists of the following four steps: CT image interpolation, pulmonary region segmentation, nodule extraction, and nodule volume measurement. Nodule extraction is performed based on the radius and CT number. The proposed method was applied to a public database (Volcano '09). We confirmed that the nodule volume measurements performed using our proposed method were successful, according to a subjective evaluation.

Keywords: Pulmonary nodule, volume measurement, CT images, Volcano '09.

1   Introduction

Radiologists often use X-ray computed tomography (CT) images for detecting or evaluating pulmonary nodules. Determining the change in the pulmonary nodule size is a critical measurement for cancer diagnosis and therapy evaluation. One of the most important indicators of malignancy is the relative change in the size of a nodule over a period of time [1]. However, during nodule size estimation, there is a large amount of variation or disagreement in size estimation, even by medical experts. It seems that quantification of nodule volume using a computer would be effective in resolving this issue. In this study, a method that quantifies the nodule size change using relatively simple image-processing techniques is proposed.

2   Method

Figure 1 shows a flowchart of our proposed method. The method consists of the following four steps: (1) interpolation of the CT images, (2) segmentation of the pulmonary region, (3) extraction of the nodule region, and (4) quantification of the nodule volume.

The proposed method is a 3D-based approach that requires an isotropic image resolution in CT images. However, the spatial resolution of CT images often differs

between pixel spacing and slice thickness. To solve this problem, CT images are interpolated into an isotropic matrix by changing the slice thickness to pixel spacing as a pre-process of the nodule region determination. After this processing, the proposed method can be adaptable to any CT images with different spatial resolutions (Z-direction).

Pulmonary nodules exist within the pulmonary region. Therefore, the pulmonary region should be segmented first. The pulmonary region consists mostly of air, and it can be easily segmented using CT number thresholding. However, if the nodules are connected to the chest wall, determining the pulmonary region may not be easy. We designed a pulmonary segmentation method applicable to the attached nodules. The proposed method can detect various types of nodules (including attached nodules), and it is designed to adapt to the nodules with 2–30 mm diameters.

The proposed method is an automated approach and requires minimum user interaction (the user is only required to locate the center point of the target nodule). We identified nodules in the high-CT number regions on the pulmonary regions. Therefore, the proposed method extracts nodules using CT number thresholding. However, making a distinction between nodules and blood vessels using CT numbers is difficult. The proposed method attempts to solve this problem by localizing the nodule existence range before gray-level thresholding.

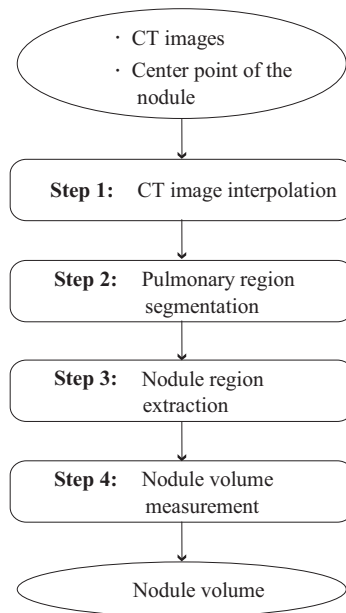The details of the proposed method are described below.

Fig. 1. Flowchart of the proposed method.

2.1   CT image interpolation

In this section, we describe an interpolation method by which each voxel on the CT images is interpolated to have isotropic dimensions. Let s be the spatial coordinates of the image, which is defined as follows:

$$s = \{(x, y, z) : 1 \le x \le w, 1 \le y \le h, 1 \le z \le d\}. \tag{1}$$

Let $f(p) \mid p \in s$ be an arbitrary image. First, the pixel spacing and slice thickness are obtained from a DICOM file header. Next, the CT images are reformatted using the following equation to conform the slice thickness to the pixel spacing.

$$f(x_0, y_0, z_0) = \sum_k \sum_l \sum_m f(x_k, y_l, z_m) C(x_k - x_0) C(y_l - y_0) C(z_m - z_0), \tag{2}$$

where (x_k, y_l, z_m) denotes the grid point around (x_0, y_0, z_0). The interpolating function C is defined as sinc function [2].

$$C(x) = \frac{\sin \pi x}{\pi x}. \tag{3}$$

Figure 2 shows an example of before and after interpolating the CT images. In this figure, a change in the slice thickness in the CT images can be recognized. In the following sections, we use $CT(p)$ to represent the interpolated CT images.

(a) Before interpolation   (b) after interpolation

Fig. 2. An example of interpolated CT images (one coronal section).

2.2   Pulmonary region segmentation

In this section, we describe a method for segmenting the pulmonary region (see Fig. 3). The pulmonary region consists mostly of air. Therefore, the pulmonary region can be identified as a region with low CT numbers on the CT images. Therefore, the proposed method extracts air regions using CT number thresholding. Threshold th H.U. is determined using the Otsu method [3]. However, the existence of noise on the CT images often causes segmentation failure. In order to reduce the noise, the CT images are smoothed using a median filter. A binary image $B(p)$ is then generated using the following equation.

$$B(p) = \begin{cases} 1 & \text{if } Med(CT(p)) < th \\ 0 & \text{otherwise} \end{cases}, \tag{4}$$

where *Med* denotes the function of the median filter.

Each air region is then labeled by applying 3D labeling processing to $B(p)$. Then, external air regions and small air regions are removed, and the pulmonary region $B'(p)$ is extracted as follows:

$$B'(p) = \begin{cases} 1 & if\ A_i = 0 \wedge \sum q \geq \alpha\ |\ q \in Label(B[p]) = i,\ 1 \leq i \leq n \\ 0 & otherwise \end{cases}, \tag{5}$$

$$A_i = \begin{cases} 1 & if\ Cir(q) = 1\ |\ q \in Label(B[p]) = i,\ 1 \leq i \leq n \\ 0 & otherwise \end{cases}, \tag{6}$$

$$Cir(p) = \begin{cases} 1 & if\ \left(x - \dfrac{w}{2}\right)^2 + \left(y - \dfrac{h}{2}\right)^2 = r^2 \\ 0 & otherwise \end{cases}, \tag{7}$$

where r voxel denotes the radius of the circle.

Holes in the pulmonary region are then filled in each slice. In particular, each voxel value of $B'(p)$ is reversed, and labeling processing is performed. Labeled regions that are not adjacent to the edge of the slice image are added to the pulmonary region. This resulting image is defined as $B''(p)$.

Finally, closing operation [4] is applied to $B''(p)$, and the binary image of the pulmonary region $B_p(p)$ is obtained.

$$B_p(p) = \left[\left(B''(p) \oplus g^s\right) \ominus g\right](p), \tag{8}$$

where $\oplus$ denotes the Minkowski sum, $\ominus$ denotes the Minkowski difference, and g denotes the structural element, which consists of a sphere with a radius of t mm.

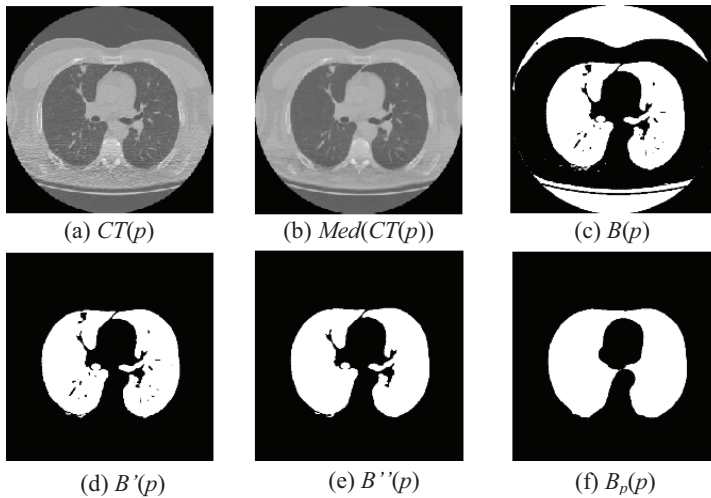| (a) $CT(p)$ | (b) $Med(CT(p))$ | (c) $B(p)$ |
| (d) $B'(p)$ | (e) $B''(p)$ | (f) $B_p(p)$ |

Fig. 3. Process flow of pulmonary region segmentation (one axial section).

2.3   Nodule region extraction

In this section, we describe a extraction method of the nodule region (see Fig. 4). First, CT number thresholding is applied to the pulmonary region, and the image $N_1(p)$ is obtained.

$$N_1(p) = \begin{cases} 1 & if \ \ Med(CT(p)) \geq th_2 \wedge B''(p) = 1 \\ 0 & otherwise \end{cases}, \tag{9}$$

where th_2 H.U. is determined by applying the Otsu method to the smoothed CT voxels with $B''(p)=1$.

Second, Euclidean distance transformation [5] is applied to $N_1(p)$, and the distance image $D(p)$ is obtained.

$$D(p) = \min_{q=(x_0, y_0, z_0) \in s} \sqrt{(x - x_0)^2 + (y - y_0)^2 + (z - z_0)^2} \mid N_1(q) = 0. \tag{10}$$

Blood vessels have a tubular-like structure, while nodules have a mass-like ("spherical") structure. Therefore, the distance value of the center of a nodule should be larger than the center of a blood vessel. Therefore, voxels within the distance value $D(c)$ are removed. Here, $c \in s$ is defined as the center point of the nodule that the user inputted. However, there is no guarantee that the user always inputs the center of the nodule. The adjusted center point $c' \in s$ is thus obtained using the following program.

```
program Optimizing center point(Input: c, Output: c')
  {c, c', c1, and c2 ∈ s,
  neighbor(p): The function which outputs the adjacent
  coordinates of the point p};
  var   c1, c2;
  begin
    c2 = c;
    repeat
      c1 = c2;
      if(D(c2) < D(neighbor(c1)))
        c2 = neighbor(c1);
      )
    until c1 = c2
    c' = c1;
  end.
```

Third, $D'(p)$ is obtained by the following equation.

$$D'(p) = \begin{cases} D(p) & if \ \ D(p) \geq D(c') \\ 0 & otherwise \end{cases}. \tag{11}$$

Fourth, $D'(p)$ is applied to reverse Euclidean distance transformation [6], and image $N_2(p)$ is obtained.

$$N_2(p) = \begin{cases} 1 & if \ d(p,q) < D'(q) | \ q \in s \\ 0 & otherwise \end{cases}, \tag{12}$$

where $d(p, q)$ is the function that outputs the Euclidean distance between points p and q.

Fifth, $N_2(p)$ is applied to labeling processing, and only the region including c' is extracted. This resulting image is defined as $N_3(p)$.

$$N_3(p) = \begin{cases} 1 & if \ Label(N_2(p)) = Label(N_2(c')) \\ 0 & otherwise \end{cases}. \tag{13}$$

If a nodule is a pure sphere, a nodule region will be extracted in $N_3(p)$. However, since a nodule is not a pure sphere, it is necessary to extend the region. At the sixth processing, the image $N_4(p)$ that extended the region is obtained.

$$N_4(p) = \begin{cases} 1 & if \ d(p,q) < D''(q) | \ q \in s \\ 0 & otherwise \end{cases}, \tag{14}$$

$$D''(p) = \begin{cases} D(p) & if \ N_3(p) = 1 \\ 0 & otherwise \end{cases}. \tag{15}$$

Seventh, the $N_4(p)$ region is applied to CT number thresholding, and the nodule region $N_5(p)$ is obtained.

$$N_5(p) = \begin{cases} 1 & if \ N_4(p) = 1 \wedge CT(p) \geq th_3 \wedge B_p(p) = 1 \\ 0 & otherwise \end{cases}, \tag{16}$$

where th_3 H.U. is the fixed threshold.

The holes in $N_5(p)$ are then filled using the abovementioned method. The resulting image is defined as $N_6(p)$. Finally, the opening operator [4] is applied to $N_6(p)$, and then, only the region including c' is extracted. Hence, the nodule region $N(p)$ is obtained.

$$N_7(p) = \left[\left(N_6(p) \ominus g_2^s \right) \oplus g_2 \right](p), \tag{17}$$

$$N(p) = \begin{cases} 1 & if \ Label(N_7(p) = Label(N_7(c'))) \\ 0 & otherwise \end{cases}. \tag{18}$$

(a) $Med(CT(p)) \cap B''(p) = 1$ (b) $N_1(p)$ (c) $D(p)$

(d) $D'(p)$ (e) $N_2(p)$ (f) $N_3(p)$

(g) $N_4(p)$ (h) $N(p)$

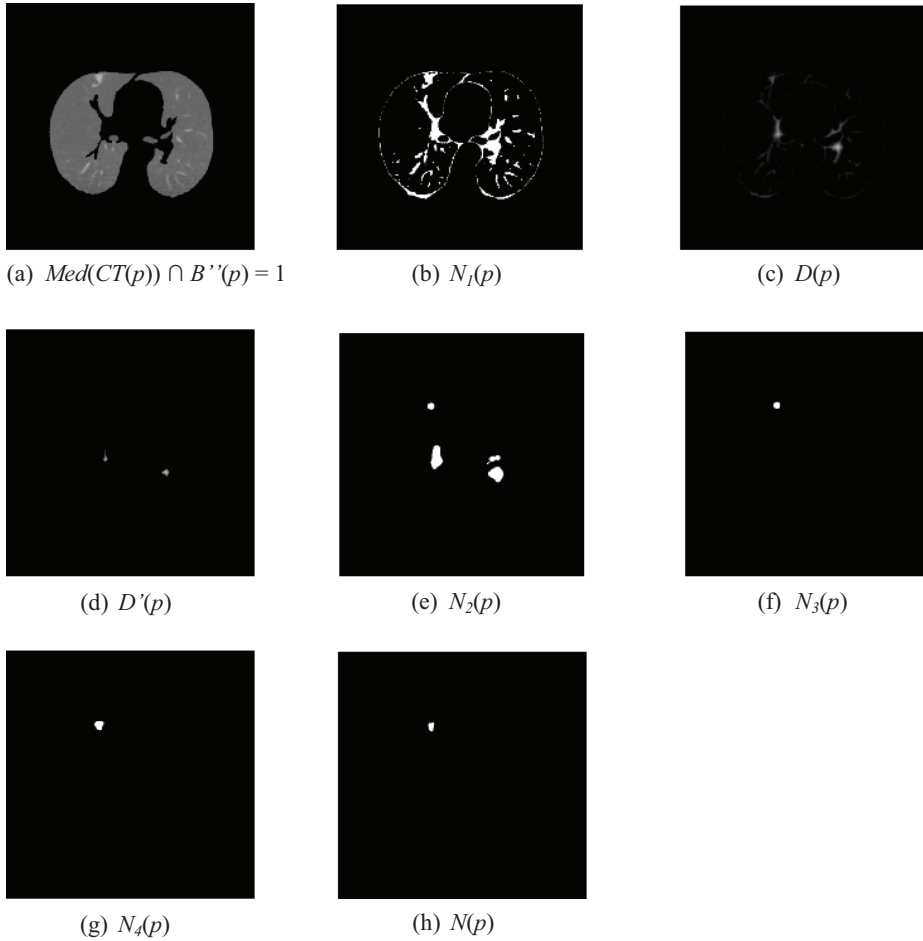**Fig. 4.** Process flow of nodule region extraction (one axial section).

2.4   Nodule volume measurement

The nodule volume V is calculated using $N(p)$ and pixel spacing.

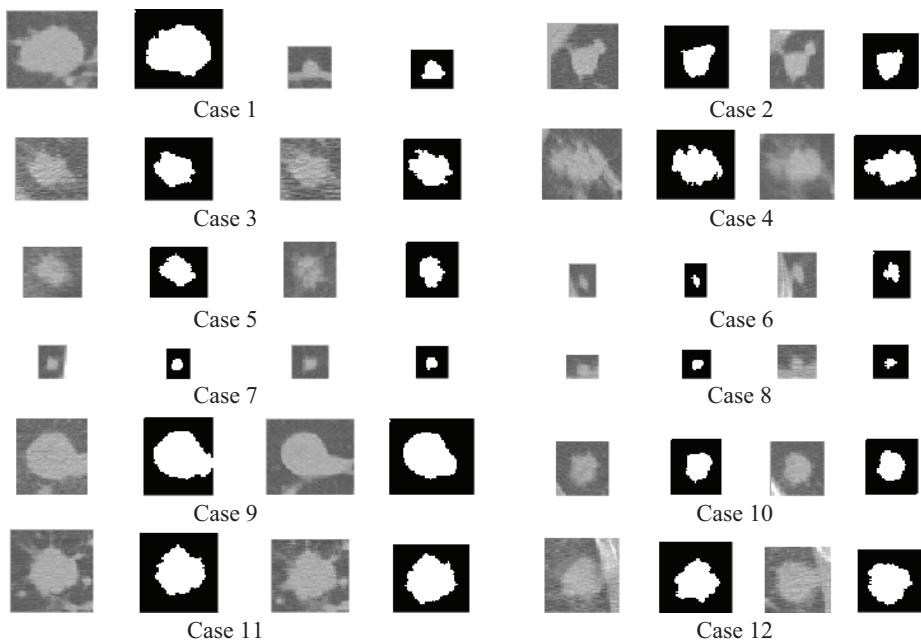$$V = \sum q \times pixel\_spacing^3 \mid q \in s \wedge N(q) = 1. \qquad \textbf{(19)}$$

3   Results

The proposed method was applied to a database known as Volcano '09. Volcano '09 consists of CT images obtained from 50 cases. Each CT case was scanned over a
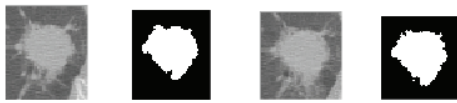
period of time. Let V_1 and V_2 be the volume of the nodules in the CT images for the first and second scans, respectively. Note that the target nodule is defined in advance. In order to quantify the nodule volume and its change, we calculated V_1, V_2, and $(V_2 - V_1)/V_1$ using the proposed method. Parameters used in the experiment were $r = 255$, $t = 15$, and $th_3 = -350$. Moreover, the smoothed image was defined as the CT image that was applied by using a median filter with a mask size of $3 \times 3 \times 3$, twice. These parameters were determined empirically.

The results of the extracted nodules are shown in Fig. 5, and the nodule volume measurement results are shown in Table 1. By carrying out a subjective evaluation, we confirmed that the nodule volume measurements were successful in most cases. However, cases in which the nodule size was small produced a large measurement error due to over- or under-extraction. For example, the outside of the pulmonary region was slightly over-extracted in the second scan in case 6. Moreover, the size of this nodule was quite small. Therefore, the value of an excessive size ratio was calculated.

It was difficult to determine the contour of the nodules in cases 30 and 31 because those nodules arose in the pulmonary hilum. Values of the CT numbers of nodules and tissues in the pulmonary hilum are almost the same; therefore, separating the nodule from the pulmonary hilum based on the CT numbers is difficult. However, the anatomical shapes of the pulmonary hilum could be used to solve this problem.

The calculation time in each case was 59 ± 21 s (CPU: Intel Core2 Duo E7200, Memory: 4 GB). A majority of the calculation cost (approximately 90%) was spent in the smoothing process. If an alternative smoothing method with low calculation cost is used instead of a method that involves the use of a median filter, the calculation cost will be reduced.
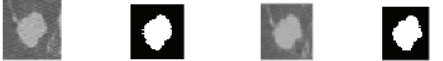

Case 1   Case 2

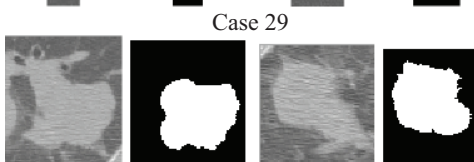Case 3   Case 4
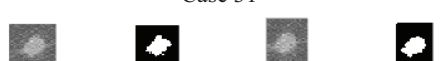
Case 5   Case 6

Case 7   Case 8

Case 9   Case 10

Case 11   Case 12

Case 13

Case 14

Case 15

Case 16

Case 17

Case 18

Case 19

Case 20

Case 21
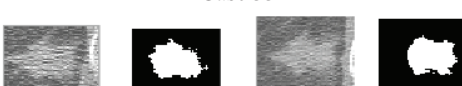
Case 22

Case 23

Case 24

Case 25

Case 26
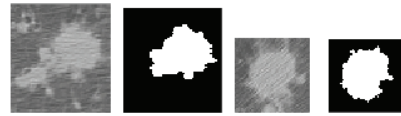

Case 27

Case 28

Case 29

Case 30

Case 31

Case 32

Case 33

Case 34

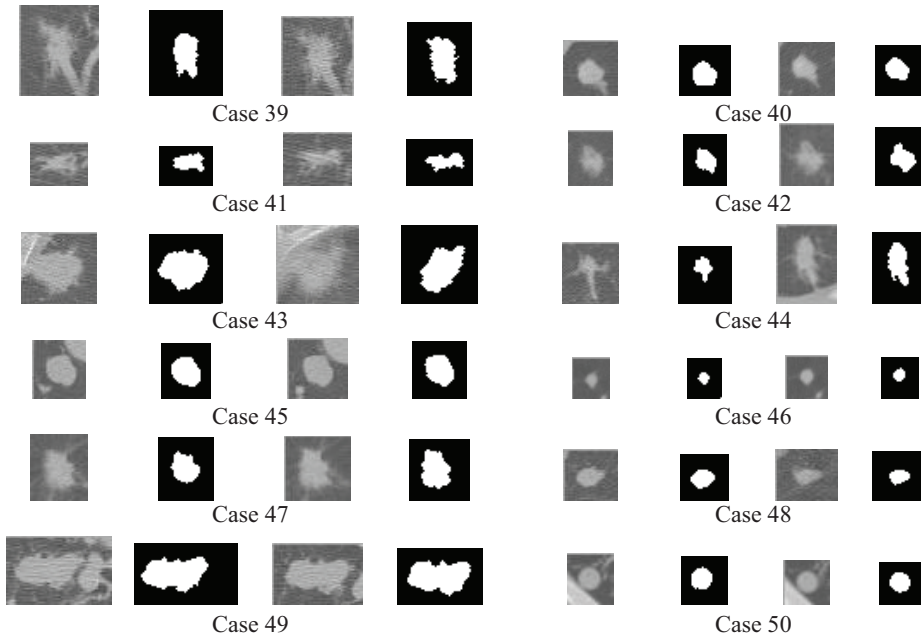Case 35

Case 36

Case 37

Case 38

Fig. 5. Nodule extraction results for all 50 cases using our proposed method (one axial section around a target nodule). From left to right, the figure shows the interpolated CT images in the first scan, the extraction results of a target nodule in the first scan, the interpolated CT images in the second scan, and the extraction results of a target nodule in the second scan.

4   Discussions

In the case of lesion size or volume estimation, there is a large amount of variation and disagreement about the results, as determined by different experts. We believe that quantitative size or volume estimation carried out using a computerized method can contribute to reduce such variation and disagreement. A computerized method with a few user interactions is desirable, because such interactions are dependent on the user's subjectivity. Therefore, we designed the proposed method that requires minimum user interaction (the user must only indicate a point near to the center of target nodule). Furthermore, the proposed method can automatically adjust the point from the position of user interventions to the "real center" of the target nodule. The position of the points from user interventions had observer variations, and the proposed method could provide results independent of those variations.

We only selected and used one feature for nodule segmentation in the proposed method, based on the experience of radiologists. That is, single CT number thresholding was used to extract high-CT number regions, which radiologists would interpret as nodule regions on CT images. However, it was difficult to discriminate the pulmonary nodules from other structures using CT number thresholding in some

Table 1. Measurement results of the volumes V1 and V2 together with the volume ratio.

CaseID	$(V2 - V1)/V1$	V1 (mm^3)	V2 (mm^3)
ST0001	−0.96	3642	161
ST0002	−0.19	1431	1153
ST0003	−0.21	1842	1461
ST0004	0.09	2155	2360
ST0005	0.11	949	1049
ST0006	2.90	26	103
ST0007	−0.44	97	54
ST0008	−0.04	36	34
ST0009	−0.30	5720	3983
ST0010	−0.02	635	622
ST0011	0.08	1452	1565
ST0012	1.06	1770	3652
ST0013	−0.02	8121	7972
ST0014	−0.18	6036	4968
ST0015	−0.33	214	142
ST0016	−0.14	170	147
ST0017	1.60	452	1175
ST0018	−0.01	1978	1949
ST0019	0.13	1610	1813
ST0020	−0.04	824	792
ST0021	−0.00	1158	1157
ST0022	0.22	284	347
ST0023	−0.05	1771	1680
ST0024	0.24	562	700
ST0025	0.18	525	620
ST0026	0.31	766	1007
ST0027	−0.09	12842	11723
ST0028	−0.33	656	443
ST0029	−0.03	26	25
ST0030	−0.16	6407	5370
ST0031	−0.12	16381	14394
ST0032	0.21	27	33
ST0033	0.06	337	357
ST0034	−0.42	86	50
ST0035	−0.01	1951	1939
ST0036	0.00	723	724
ST0037	0.17	688	802
ST0038	0.04	1157	1202
ST0039	−0.19	718	582
ST0040	−0.17	498	413
ST0041	0.08	458	493
ST0042	0.46	200	292
ST0043	0.09	1794	1953
ST0044	2.31	207	684
ST0045	0.07	457	490
ST0046	0.06	59	62
ST0047	0.40	504	704
ST0048	−0.47	317	168
ST0049	−0.08	2578	2372
ST0050	−0.10	953	857

attached nodules or nodules with blood vessels. Therefore, the proposed method attempted to determine the nodules' boundaries based on their shape (radius). This approach produced appropriate results in most of the cases, as shown in Fig. 5. However, there were some cases with over-extraction results (e.g., the first scan in case 47) or under-extraction results (e.g., in cases 30 and 31). Designing a complicated method, such as a specialized scheme for nodule shapes or types of circumference tissues, may be required in order to improve the segmentation accuracy of the nodule.

Some features are assumed to be effective in nodule size estimation, including radius, major/minor axis, the nodule area in its center slice, and so on. This research used the voxel number of the 3D volume of nodules to measure the change in the nodule size because the 3D volume can accurately reflect the shape of the different nodules. The other features derived from the 3D volume, such as the degree of sphericity, should also be effective for nodule diagnosis and therapy evaluation.

5   Summary

In this study, a method that quantifies the nodule volume change by using relatively simple image-processing techniques was proposed. The nodule extraction was performed based on radius and CT number. The proposed method was applied to a database known as Volcano '09. By carrying out a subjective evaluation at an initial stage, we confirmed that the nodule volume measurements were successful.

Acknowledgments

References

1. VOLCANO'09 Challenge, http://www.via.cornell.edu/challenge/index.html
2. Tamura, H.: Computer Image Processing, 127, Ohmsha (2002) (in Japanese)
3. Otsu, N.: A threshold selection method from gray-level histograms. IEEE Trans. Systems Man Cybernet, 9 (1), 62-69 (1979)
4. Kobatake, H.: Morphology, Corona (1996) (in Japanese)
5. Saito, T., Toriwaki, J.: Euclidean distance transformation for three dimensional digital images. IEICE D-II, J76-D-II (3) 445-453 (1993) (in Japanese)
6. Saito, T., Toriwaki, J.: Reverse Euclidean distance transformation and extraction of skeletons in the digital plane. IEICE Technical Report, Pattern Recognition and Understanding, 93 (228): 57-64 (1993) (in Japanese)